

# On the Mechanism of the H–D Exchange Reaction in Ethane over Platinum Catalysts

Alfonso Loaiza,<sup>1</sup> Mingde Xu, and Francisco Zaera<sup>2</sup>

*Department of Chemistry, University of California, Riverside, California, 92507*

Received August 25, 1995; revised November 22, 1995; accepted November 29, 1995

The catalytic exchange of hydrogen atoms for deuteriums in ethane was studied over a platinum foil between 540 and 640 K by using a closed-loop microbatch reactor with mass spectrometry detection. An activation energy of 27.1 kcal/mol and kinetic orders of  $-0.55$  and  $1.00$  with respect to deuterium and ethane, respectively, were obtained on the platinum foil, in agreement with previous reports on other forms of platinum. The focus of this study was on the identification of surface intermediates by performing a detailed analysis of the resulting products. The exchange product distribution was in all cases U-shaped, with maxima at the singly and fully deuterated ethane molecules, again the same as on supported platinum catalysts and on platinum films and (111) single crystals. The uniqueness of the work reported here is that it describes the first complete quantitative determination of the distribution of symmetric and asymmetric deuterium-substituted products. In particular,  $^{13}\text{C}$ -NMR was used to determine that the yield for  $\text{CH}_2\text{D}-\text{CH}_2\text{D}$  is more than twice that for  $\text{CH}_3\text{CHD}_2$ , a result that suggests that adsorbed ethylene is one of the main intermediates in the mechanism for complete exchange. A sequence of steps that includes the formation of ethyl, ethylene, and ethylidyne surface intermediates is discussed. © 1996 Academic Press, Inc.

## 1. INTRODUCTION

In spite of the importance of the conversion of alkanes on metal catalysts in petrochemistry and other industrial processes, the mechanisms of those reactions are still far from understood. One of the main roadblocks in the study of the chemistry of saturated hydrocarbons on solid surfaces is the low probability of alkanes sticking on those substrates upon collision. Indeed, it is widely believed that most alkane activation reactions start and are kinetically limited by the dissociative adsorption of the gas-phase molecules (1–3). In order to get information about that step, several groups have focused on the study of exchange reactions where the hydrogen atoms of the hydrocarbon are replaced by deuteriums (4–10). The initial idea was to use the H–D ex-

change processes as direct probes for the adsorption, but it was soon realized that the mechanism for those reactions was more complex than initially suspected. For one, different product distributions are obtained depending on the nature of the catalyst used, from cases where the formation of monosubstituted alkane dominates, to situations where complete exchange is preferred. Perhaps the most interesting result from those studies, however, is that metals such as zirconium, chromium, vanadium, nickel, and platinum yield bimodal distributions with maxima at the mono- and perdeuteroalkanes (4). Even though such behavior does hinder the direct extrapolation of kinetic data from the exchange processes to the dissociative adsorption step, it opens new interesting avenues for the study of adsorbed intermediates during hydrogenation–dehydrogenation reactions in hydrocarbons.

A particular example of the bimodal distributions resulting from H–D exchange reactions is that of the catalytic conversion of ethane with deuterium on platinum surfaces, which predominantly yields  $d_1$ - and  $d_6$ -ethanes (4, 5, 11). In order to explain such a distribution, Anderson and Kemball proposed the occurrence of two different and independent reaction pathways on two separate types of catalytically active sites (4). They suggested a common first step for both paths, namely, the dissociative adsorption of ethane to ethyl groups on the surface. According to their mechanism, those alkyl intermediates then rehydrogenate (redeuterate) immediately on one type of sites to produce new ethane molecules (the  $d_1$  product), but dehydrogenate further in a series of steps leading to the exchange of all their hydrogen atoms before desorption on other surface locations (4). They also stipulated that the latter process may occur via the repeated interconversion between the adsorbed alkyl and a 1,2-diadsorbed alkene.

In order to test the ideas put forward by Kemball, several studies have focused on the isolation and/or identification of the possible reaction intermediates during these exchange reactions. For one, the chemistry of stable chemisorbed species such as acetylides, acetylenes, vinylidenes, vinyls, olefins, alkylidynes, and alkyls have all been characterized extensively by using modern sensitive surface techniques

<sup>1</sup> Permanent address: Departamento de Química, Universidad de Los Andes, Mérida, Venezuela.

<sup>2</sup> To whom correspondence should be addressed.

(12–23). However, the specific role that those species may play in the H–D catalytic exchange has not yet been established. A more indirect method for obtaining mechanistic information on this reaction is by determining the position at which the deuterium substitutions take place within the alkane molecule, which in the case of ethane reduces to measuring the relative yields for symmetric versus asymmetric substitutions in the  $d_2$ -,  $d_3$ -, and  $d_4$ -ethanes produced. That information can then be used to infer the structure of the surface intermediates from which those compounds originate. Unfortunately, past studies using this approach have only had a limited success (4, 24, 25).

The main objective of the work reported here was to characterize the distribution of the products obtained from ethane H–D exchange reactions on platinum foils and to relate that information to the mechanism of that reaction. A secondary goal was to develop a reliable analytical method for analyzing the gas-phase deuterium-substituted alkane mixtures that result from the exchange process. Kinetic measurements for this reaction on the platinum foil yielded an activation energy of 27.1 kcal/mol, first and negative-half orders on ethane and deuterium partial pressures, respectively, and a U-shaped product distribution with maxima at ethanes with one and six deuterium substitutions, the same as on other forms of platinum (4, 5, 11, 26, 27). In addition, both mass spectrometry and NMR were used to determine the complete make-up of the gas-phase products.  $^{13}\text{C}$ -NMR (125.76 MHz) in particular indicated that, between the  $d_2$ -ethanes, the symmetric  $\text{CH}_2\text{DCH}_2\text{D}$  was produced preferentially over the asymmetric  $\text{CH}_3\text{CHD}_2$ , the ratio between the two being about 2.3 : 1. This suggests that ethylene is an important surface intermediate in the mechanism for the complete exchange of normal ethane to perdeuteroethane. Other mechanistic details for that reaction were inferred from the kinetic data obtained in these studies as well.

## 2. EXPERIMENTAL

The experiments reported here were done in a stainless-steel microbatch reactor linked through a 1.0-m-long capillary tube to a computer-interfaced Dycor MA-200M quadrupole mass spectrometer, as shown schematically in Fig. 1. The reactor consists of a close loop of 0.20 l total volume connected to a metal bellows pump (Metal Bellows Corp., MB-21) for continuous gas circulation, a MKS Baratron vacuum gauge (PDR-C-1B) for gas pressure measurements, and a gas-inlet manifold. A platinum foil (Aldrich, 99.99% purity), 0.1 mm thick and of 1.12  $\text{cm}^2$  total area, was used as the catalyst. This sample was heated resistively to a constant temperature, which was measured by a chromel–alumel thermocouple spotwelded to the sample and continuously regulated using a precision temperature controller (Eurotherm Corp.) during the catalytic runs. Research purity ethane (Matheson, 99.96%),  $1\text{-}^{13}\text{C}$ -ethane

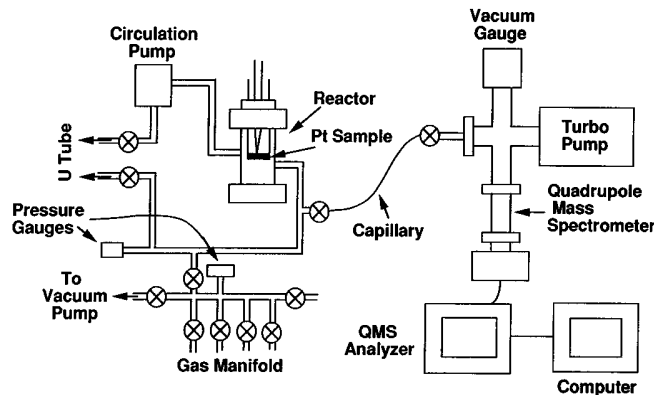


FIG. 1. Schematic diagram of the microbatch reactor used for the experiments reported here. The left-hand side shows the main loop, which includes the small volume where the platinum sample resides, a recirculation pump, a pressure gauge, and a gas manifold. Also shown are the gas sample outlets, a capillary tube to the low-resolution mass spectrometer, and a U-tube used to transfer the gas to other mass spectrometry and NMR instruments.

(CIL, 99%), and deuterium (Matheson, 99.5 atom purity) were used as supplied. Other  $d_1$ – $d_6$  deuterated ethanes (Merck-Canada, CIL, and Matheson, 99% atom purity), employed as standards in the calibration of both the mass spectrometer and the NMR signals, were also used without further treatment.

The Pt foil was cleaned before each catalytic run by exposing it sequentially to oxygen at 1075 K for 15 min and to hydrogen at 1225 K for 30 min. The sample was subsequently kept under vacuum at 1225 K for another 10 min. to desorb the remaining water, oxygen, and hydrogen from the surface, and allowed to cool down to room temperature. Ethane and deuterium were then introduced in that order to the desired pressures and circulated for 2–3 min to ensure adequate mixing, and the catalyst was heated to the reaction temperature. The progress of the exchange reaction was followed mass spectrometrically by continuously leaking the gas mixture during the experiments into the mass spectrometer via the interconnecting capillary tube. This continuous gas leak from the reaction loop to the analyzer did not affect the gas composition in the reactor to any significant level; it only led to a total pressure drop in the loop of about 1–2% over the time period of the complete experiment. The electron energy of the ionizer in the mass spectrometer was set to 70 eV, and the ion intensities were measured by a Faraday cup. The product distributions were calculated by deconvolution of the raw data using the experimental mass spectra obtained with our system for each of the pure deuterated ethanes and for several mixtures of known composition. The mass spectrometer signal intensities were also calibrated in order to obtain absolute values for the partial pressures of each component in the reaction loop.

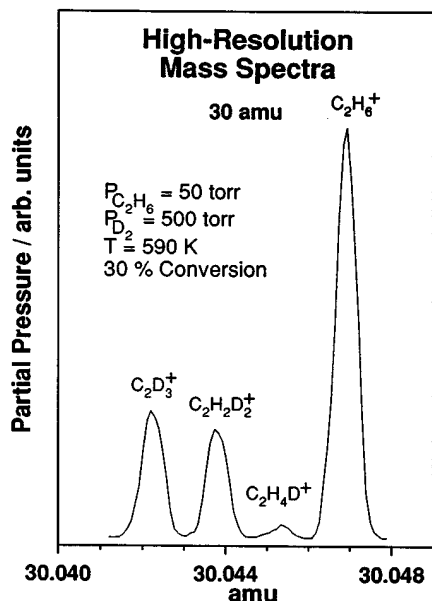


FIG. 2. Typical high-resolution mass spectrometry results from analysis of H-D exchanged ethane samples. The 30 amu region shown here illustrates how the separation of peaks from different ions ( $C_2D_3^+$ ,  $C_2H_2D_2^+$ ,  $C_2H_4D^+$ ,  $C_2H_6^+$ ) is accomplished.

More detailed analysis of the reaction mixtures were performed by using high-resolution mass spectrometry (HR-MS), tandem mass spectrometry/collision-induced decomposition mass spectrometry (MS/CID-MS), and nuclear magnetic resonance spectroscopy (NMR). For this, the gas mixtures were trapped after reactions into a U-shaped glass tube with valves at each end by means of liquid nitrogen cooling, and pumped while frozen in order to remove the hydrogen and deuterium gases from the mixture. Some samples were then leaked into a Finnigan-MAT 900 high-resolution mass spectrometer operated at 70 eV ionization energy and source temperature of 180°C. The static resolving power of that instrument (amu value over full-width at 10% of maximum) was set to approximately 25,000 by using a 1:9 mixture of benzene:pyridine and resolving the 79 amu doublet. This was sufficient to separate the different isotopically-substituted ionic fragments. Figure 2 displays typical HR-MS data obtained for the 30 amu region to illustrate this point: the signals from  $C_2H_6^+$ ,  $C_2H_4D^+$ ,  $C_2H_2D_2^+$ , and  $C_2D_3^+$  are clearly separated in this spectrum. Such resolution allowed for the direct measurement of the sample composition without the need of applying any deconvoluting routine (as in the low-resolution experiments).

A second set of gas samples was analyzed by utilizing a VG ZAB 2FHF high-resolution reversed-geometry mass spectrometer for tandem MS/CID-MS detection. The first stage was equipped with an electron-impact ionizer set at 70 eV ionization energy, 200°C source temperature, and a resolving power of 1000. MS/MS spectra were obtained

by filtering the ion of interest with the first electromagnet and passing the resulting beam through an atmosphere of  $5.5 \times 10^{-6}$  Torr helium in the intermediate field-free region before sending it to the second stage in order to induce its fragmentation via gas-phase collisions.

Finally, a third group of samples was analyzed by NMR, by transferring the gas mixtures into 5-mm-wide NMR glass tubes containing 0.5 ml of deuterated chloroform (Aldrich, 99.9% atom D), which were then sealed. All  $^1H$ -,  $^2H$ -, and  $^{13}C$ -NMR were obtained by using a General Electric GN-500 NMR spectrometer equipped with a home-built X-nucleus decoupler and a Z-spec 5 mm inverse detection broadband probe. The  $^{13}C$ -NMR spectra were collected as 16 K complex data points with an operating frequency of 125.763 MHz and a sweep width of 11,364 Hz, and with the  $^1H$  and  $^2H$  decoupling channels gated on. In order to increase the signal-to-noise ratio in the  $^{13}C$ -NMR spectra,  $1\text{-}^{13}C$  labeled ethane was utilized in the catalytic runs for those experiments.

### 3. RESULTS

The catalytic exchange of hydrogen atoms for deuterium in ethane over a platinum foil was investigated at temperatures between 540 and 640 K. Pressures of 500 Torr of deuterium and 50 Torr of ethane were used in these experiments unless otherwise indicated. Figure 3 shows typical product

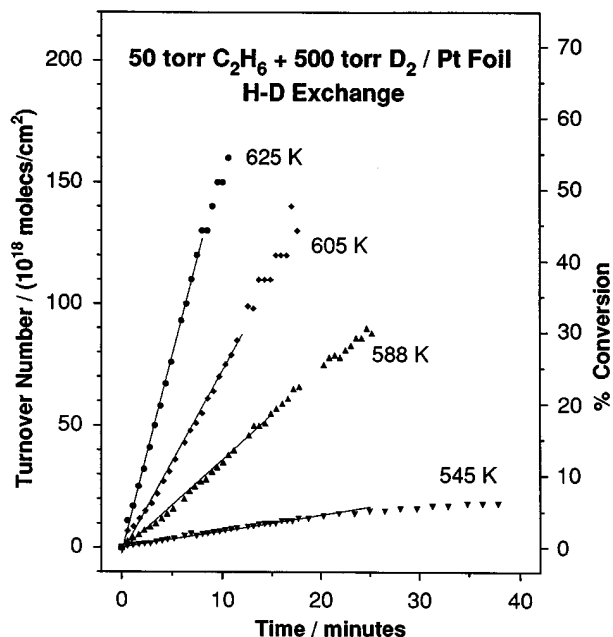


FIG. 3. Total product accumulation curves as a function of time from H-D exchange in ethane over a platinum foil at 545, 588, 605, and 625 K. The symbols represent the experimental data (obtained by following the disappearance of the light alkane), while the solid lines are the result of fits to a first-order rate law; 50 Torr of normal ethane and 500 Torr of deuterium were used in all runs.

TABLE 1

Dependence of the Initial Reaction Rates for the Catalytic H-D Exchange in Ethane over a Platinum Foil on Both Temperature and Reactant Partial Pressures

$T$ (K)	$P_{C_2H_6}$ (Torr)	$P_{D_2}$ (Torr)	Specific activity ( $10^{17}$ molecules/cm <sup>2</sup> ·s)
545	50	500	0.11
558	50	500	0.18
588	50	500	0.62
605	50	500	1.25
625	50	500	2.68
625	30	500	1.25
625	10	500	0.48
625	50	1000	1.71
625	50	1500	1.48
Summary			
$E_a$ (kcal/mol)	$\log A^a$	$a^b$	$b^b$
$27.1 \pm 1.5$	$26.9 \pm 2.0$	$-0.55 \pm 0.03$	$1.04 \pm 0.15$

<sup>a</sup> A stands for preexponential factor, in molecules/cm<sup>2</sup> · s.

<sup>b</sup> Orders in deuterium (*a*) and ethane (*b*) partial pressures.

accumulation curves, obtained by following the disappearance of the light alkane ( $d_0$ ), for four different reaction temperatures. The initial reaction rates, calculated both from the slopes of those curves at time zero and by fitting the data to a first-order rate law, are reported in Table 1. An Arrhenius analysis of those values, shown in Fig. 4, resulted in an estimated activation energy of about  $27.1 \pm 1.5$  kcal/mol. Figure 5 shows raw kinetic data for reactions carried out at 625 K and different ethane and deuterium partial pressures, and Table 1 lists the calculated initial reaction rates from those runs as well. The rates were found to be approximately proportional to the partial pressure of ethane and inversely proportional to the square root of the deuterium pressure. A summary of the main kinetic parameters obtained for the H-D exchange is given in Table 1.

Even though the linear dependence of the reaction rates on ethane pressure justifies the first-order model used for initial rate calculations (solid lines in Fig. 3), it was noted that the fits do deviate slightly from the experimental points at high conversions. Restart experiments with fresh gas mixtures but over used catalysts (without cleaning the sample between experiments) were performed to check on the stability of the platinum foil over time. It was found that the initial activities measured in those experiments amounted to only approximately 80–90% of those of the clean surfaces. This indicates that the sample becomes slowly poisoned over time.

The composition of the product mixtures resulting from ethane H-D exchange reactions was characterized further by using both mass spectrometry and NMR. Figure 6 shows a comparison between the low- and high-resolution mass spectrometry data obtained at the end of a typical run. Even

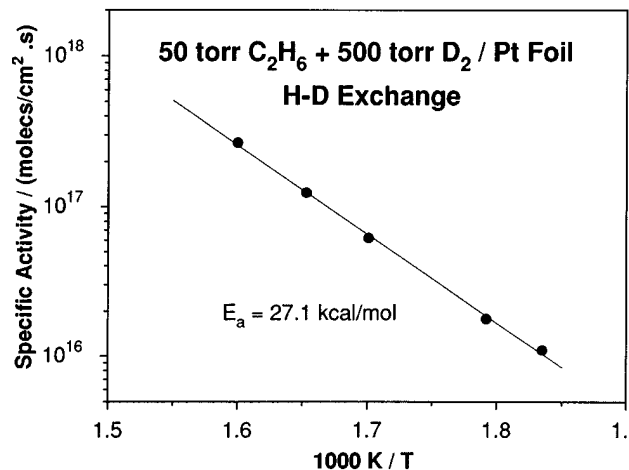


FIG. 4. Arrhenius plot of the initial reaction rates obtained from the data in Fig. 3 as a function of temperature. An apparent activation energy of  $27.1 \pm 1.5$  kcal/mol was calculated from this graph.

though the low-resolution data tends to overestimate the amount of light ethanes produced, it reproduces the overall conversion and the general distribution curve reasonably well. A U-shaped distribution was found in all cases, with maxima at one ( $d_1$ ) and six ( $d_6$ ) and a minimum at three ( $d_3$ ) atoms per ethane molecule. Furthermore, in spite of the systematic differences between the low- and high-resolution mass spectrometric results, the data obtained with the former technique was proven reliable for identifying trends in product distribution changes with changing reaction conditions. It was shown that this distribution does indeed change slightly with reaction time, reaction temperature, and partial pressures. Figure 7, for instance, shows how the distribution evolves over time: four product profiles, recorded between 6 and 10 min (between about 30 and 50% conversion) after the start of a reaction carried out at 625 K, are displayed. Two general trends were observed with increasing time: (i) the production of fully deuterated ethane ( $d_6$ ) is always favored over monodeuterated ( $d_1$ ) production, and (ii) the yield for dideutero ethane ( $d_2$ ) increases relative to any other type of ethane. More  $d_6$  and less  $d_1$  and  $d_2$  production was observed when the reaction temperature was increased (Fig. 8), and a sharpening in the distribution because of an enhancement in the combined yield for  $d_1$  and  $d_6$  was obtained by increasing the deuterium-to-ethane ratio, either by increasing the deuterium partial pressure or by decreasing that of ethane (Fig. 9). Other subtle differences were seen in the latter studies depending on the specific pressures used.

Figure 10 shows the <sup>13</sup>C-NMR spectrum of the product mixture obtained after reacting 50 Torr of 1-<sup>13</sup>C-ethane with 500 Torr of deuterium at 625 K over our platinum foil. <sup>13</sup>C-NMR is a technique ideally suited for discriminating between symmetrically and asymmetrically substituted

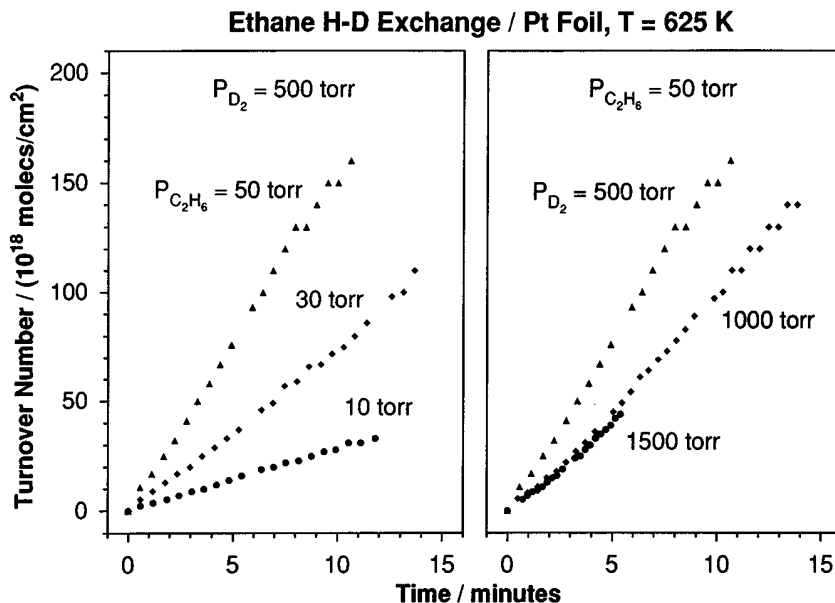


FIG. 5. Total product accumulation curves as a function of time from H-D exchange in ethane over a platinum foil illustrating the rate dependence of the partial pressures of the reactants. The left panel displays results from runs where the pressure of deuterium was kept constant at 500 Torr while that of ethane was varied between 10 and 50 Torr; the right panel shows data for experiments with 50 Torr of ethane and between 500 and 1500 Torr of deuterium. Analysis of these curves yielded  $1.04 \pm 0.15$  and  $-0.55 \pm 0.03$  orders on ethane and deuterium partial pressures, respectively. All runs were performed at 625 K.

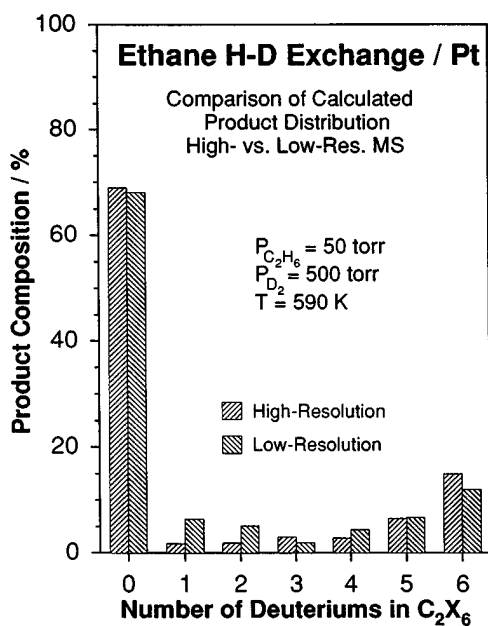


FIG. 6. Comparison between high- and low-resolution mass spectrometry analysis of the reaction mixture after about 30% H-D exchange (about 25 min) between 50 Torr of normal ethane and 500 Torr of deuterium over a platinum foil at 590 K. Both techniques reproduce the main features of the composition of the sample reasonably well; namely, they provide comparable estimates for the amount of total conversion and yield bimodal product distributions. However, the low-resolution instrument overestimates somewhat the amount of light alkanes produced.

molecules with the same total number of deuterium atoms, because the level of deuterium substitution on a molecule causes an appreciable chemical shift to lower values in the carbon signals. By using a collection of pure deuterated ethanes it was found that this effect increases linearly and

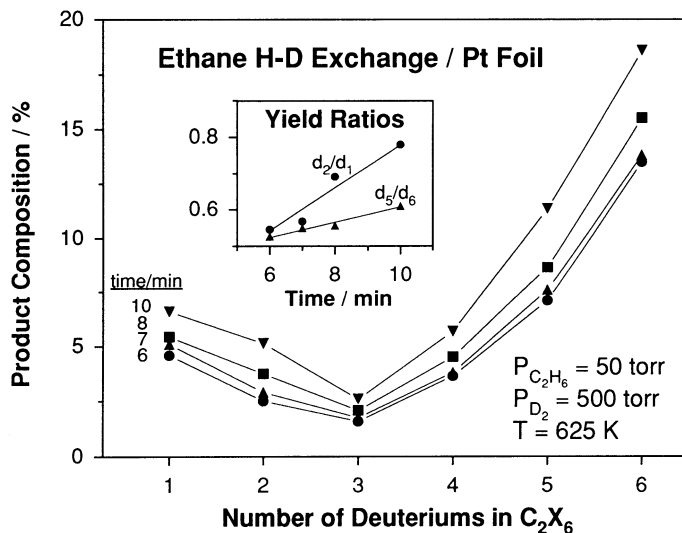


FIG. 7. Product distributions for the gas mixture of an ethane H-D exchange run on a platinum foil at different times during the course of the reaction. To notice here are the relative increases in  $d_2$ - and  $d_6$ -ethane production with time (the  $d_2/d_1$  and  $d_5/d_6$  ratios are shown in the inset). The initial mixture was composed of 50 Torr of normal ethane and 500 Torr of deuterium, and the reaction was carried out at 625 K.

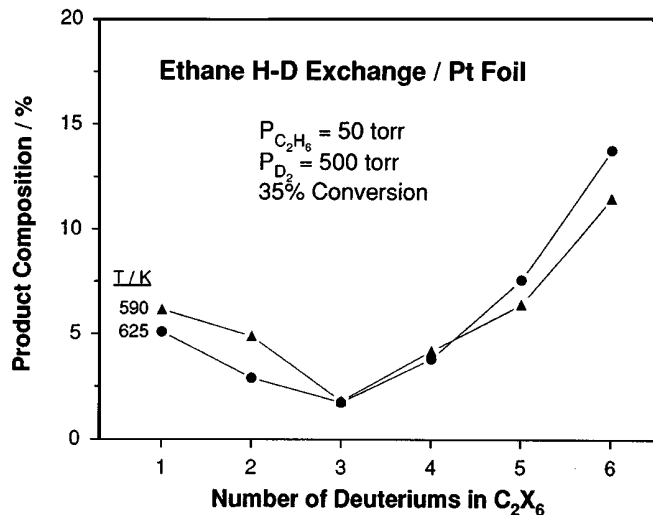


FIG. 8. Product distributions obtained after reaching a 35% conversion in-ethane H-D exchange runs on a platinum foil at 590 and 625 K. A selectivity toward the production of light alkanes at low temperatures,  $d_2$ -ethane in particular, is seen relative to the preference for  $d_6$  production at higher temperatures. Initial conditions: 50 Torr normal ethane and 500 Torr deuterium.

in an additive fashion with the number of substitutions: shifts of approximately 290 and 100 ppb were measured for each deuterium substitution on the primary and secondary carbons in ethane, respectively (28–30). The results of a quantitative analysis of the data for the reaction mixture, after having made the appropriate peak assignments, is given in Table 2. The  $^{13}C$ -NMR analysis of the reaction products shows the same U-shaped distribution with maxima at one and six deuterium atoms and minimum at three obtained by mass spectrometry, but it does deviate in a few instances from the results from low-resolution mass spectrometry (compare the last two columns of Table 2), again highlighting the shortcomings of the latter technique for the analysis of small amounts of light ethanes in these mixtures. Of particular importance to the coming discussion is the observation that the yield for the symmetrically substituted  $CH_2DCH_2D$  dideuterated ethane was about 2.3 times that of  $CH_3CHD_2$ . Also, the formation of  $CH_3CD_3$  was negligible compared to that of the asymmetric  $CH_2DCHD_2$ , and the production  $d_4$ -ethane was split almost statistically between the symmetric and asymmetric isomers.

Mass spectrometry was used to corroborate the results obtained with NMR. Due to the experimental uncertainties in the cracking patterns of the pure substances and the nature of our samples (which contain only a few percent of  $d_2$  mixed with large quantities of  $d_0$  and  $d_6$ ), however, the separation between symmetrically and asymmetrically substituted molecules by straight high-resolution mass spectrometry was not possible (31). The use of tandem MS/MS, on the other hand, did help in establishing the lack of any significant amount of the asymmetric  $d_2$  isomer in the

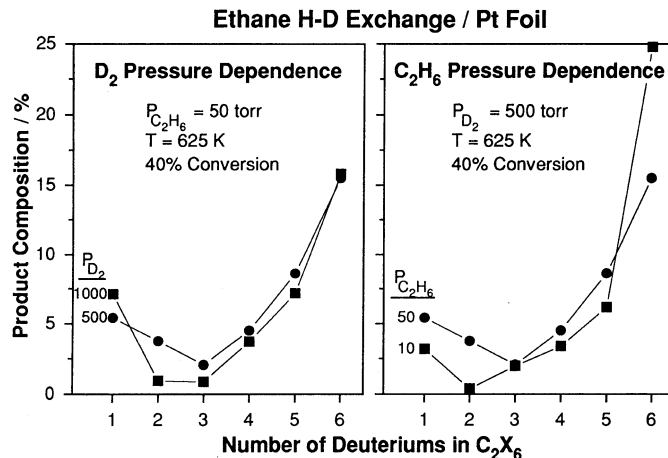


FIG. 9. Product distributions obtained after a 40% conversion of ethane in H-D exchange runs on a platinum foil at 625 K and with different initial reaction mixtures. The left panel displays the changes observed when switching from 500 to 1000 Torr of deuterium, while the right panel shows the results in going from 50 to 10 Torr of ethane. In both cases, the main change observed is that the distributions become sharper, reaching a larger combined yield for  $d_1$ - and  $d_6$ -ethane with increasing deuterium-to-ethane ratio.

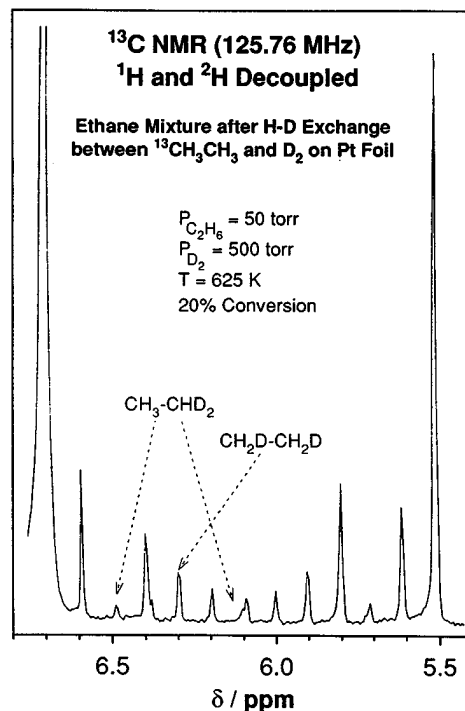


FIG. 10.  $^{13}C$ -NMR spectrum from an ethane mixture obtained after about 5 min of reaction between 50 Torr of  $1-^{13}C$ -ethane and 500 Torr of deuterium over a platinum foil at 625 K (20% conversion). Well-spaced peaks are seen for each type of carbon atom depending on the number of deuterium and  $CH_xD_{3-x}$  substitutions. The signals corresponding to the symmetrically and asymmetrically substituted  $d_2$ -ethanes are also indicated in the figure as examples of the peak assignment. A complete quantitative analysis of the reaction mixture based on this spectrum is provided in Table 2.

TABLE 2  
<sup>13</sup>C-NMR Data from an Ethane Mixture Obtained after Reacting 50 Torr  
of <sup>13</sup>CH<sub>3</sub>CH<sub>3</sub> and 500 Torr of D<sub>2</sub> over a Platinum Foil at 625 K

Species	NMR signal	NMR δ <sup>13</sup> C (ppm)	Concentration (% total)	
			From NMR	From LR-MS <sup>a</sup>
<i>d</i> <sub>0</sub> : CH <sub>3</sub> CH <sub>3</sub>	<sup>13</sup> CH <sub>3</sub> CH <sub>3</sub>	6.700	81.5	79.5
<i>d</i> <sub>1</sub> : CH <sub>3</sub> CH <sub>2</sub> D	<sup>13</sup> CH <sub>3</sub> CH <sub>2</sub> D	6.600	2.8	5.8
	CH <sub>3</sub> <sup>13</sup> CH <sub>2</sub> D	6.410		
<i>d</i> <sub>2</sub> asym.: CH <sub>3</sub> CHD <sub>2</sub>	<sup>13</sup> CH <sub>3</sub> CHD <sub>2</sub>	6.499	0.3	0.6
	CH <sub>3</sub> <sup>13</sup> CHD <sub>2</sub>	6.119		
<i>d</i> <sub>2</sub> sym.: CH <sub>2</sub> DCH <sub>2</sub> D	<sup>13</sup> CH <sub>2</sub> DCH <sub>2</sub> D	6.310	0.7	
<i>d</i> <sub>3</sub> asym.: CH <sub>3</sub> CD <sub>3</sub>	<sup>13</sup> CH <sub>3</sub> CD <sub>3</sub>	6.403	0.1	0.9
	CH <sub>3</sub> <sup>13</sup> CD <sub>3</sub>	5.828		
<i>d</i> <sub>3</sub> sym.: CH <sub>2</sub> DCHD <sub>2</sub>	<sup>13</sup> CH <sub>2</sub> DCHD <sub>2</sub>	6.210	0.7	1.4
	CH <sub>2</sub> D <sup>13</sup> CHD <sub>2</sub>	6.020		
<i>d</i> <sub>4</sub> asym.: CH <sub>2</sub> DCD <sub>3</sub>	<sup>13</sup> CH <sub>2</sub> DCD <sub>3</sub>	6.106	0.7	3.7
	CH <sub>2</sub> D <sup>13</sup> CD <sub>3</sub>	5.726		
<i>d</i> <sub>4</sub> sym.: CHD <sub>2</sub> CHD <sub>2</sub>	<sup>13</sup> CHD <sub>2</sub> CHD <sub>2</sub>	5.919	0.7	
<i>d</i> <sub>5</sub> : CHD <sub>2</sub> CD <sub>3</sub>	<sup>13</sup> CHD <sub>2</sub> CD <sub>3</sub>	5.820	3.8	
	CHD <sub>2</sub> <sup>13</sup> CD <sub>3</sub>	5.630		
<i>d</i> <sub>6</sub> : CD <sub>3</sub> CD <sub>3</sub>	<sup>13</sup> CD <sub>3</sub> CD <sub>3</sub>	5.530	8.7	8.1

<sup>a</sup> Low-resolution mass spectrometry.

reaction mixtures. Key results from this analysis are shown in Fig. 11. Here, the 32 amu ions (C<sub>2</sub>H<sub>4</sub>D<sub>2</sub><sup>+</sup>, C<sub>2</sub>H<sub>2</sub>D<sub>3</sub><sup>+</sup>, and C<sub>2</sub>D<sub>4</sub><sup>+</sup>) were picked from the mass spectra obtained in the first stage (insets), and fragmented and filtered again to obtain the secondary pattern displayed in the large panels. A comparison between spectra from the reaction mixture and from pure CH<sub>3</sub>CHD<sub>2</sub> immediately points to the absence of the latter compound in the former sample. Specifically, note the lack of any significant signal for 17 amu ions (CD<sub>2</sub>H<sup>+</sup>) in the spectrum of the mixture. That peak is a signature feature in the spectrum for 1,1-*d*<sub>2</sub>-ethane, because the other possible routes for its production (the cracking of CHD<sub>2</sub>CHD<sup>+</sup> ions originating from CHD<sub>2</sub>CHD<sub>2</sub> and CHD<sub>2</sub>CH<sub>2</sub>D) have much lower cross sections (31).

Finally, a few additional kinetic runs were performed with mixtures of perdeuteroethane and normal hydrogen. Results from a typical run, both kinetic data and the final product distribution, are displayed in Fig. 12. The results from these experiments are qualitatively consistent with those obtained with C<sub>2</sub>H<sub>6</sub> + D<sub>2</sub> mixtures. There does seem to be an enhanced preference for multiple exchange when starting with deuterated ethane, but this may be the result of the higher temperatures used in the runs with the labelled ethane. An activation energy of about 27.6 kcal/mol was obtained for the exchange in C<sub>2</sub>D<sub>6</sub>, the same within experimental error as in normal ethane.

#### 4. DISCUSSION

The intention of the work described in this paper was to use detailed kinetic information on the catalytic H-D

exchange of alkanes to unravel some of the mechanistic details of those reactions. In particular, the catalytic exchange in ethane over a platinum foil was studied between 540 and 640 K. The results obtained here compare favorably with those of other authors (5, 11, 26, 27, 32). For instance, the value of -0.55 for the order of the reaction rate on deuterium partial pressure obtained on the foil matches those reported both on Cab-O-Sil supported catalysts (27) and on platinum (111) single-crystal surfaces (11). Furthermore, U-shaped curves similar to those shown in Figs. 6, 7, 8, and 9 were found in all the previous studies of this reaction on platinum substrates where the product distribution was characterized (4, 5, 11, 26, 32). Only the activation energy obtained here for the platinum foil seems to be a bit high, but the wide spread in the numbers reported in the past makes this parameter unreliable for reactivity comparisons anyway. We will return to this point later in the discussion.

The main goal of the research presented here was to determine the product distribution obtained under different reaction conditions in order to infer the possible surface intermediates responsible for the formation of such gas-phase molecules. Besides the fact that it was possible to reproduce the U-shaped distribution previously reported by other authors, the key result from this investigation is the finding that the *d*<sub>2</sub>-substituted ethane produced by H-D exchange in normal ethane is predominantly in the form of the symmetrically substituted CH<sub>2</sub>DCH<sub>2</sub>D isomer (Fig. 10 and Table 2). This observation has important implications for the mechanism of the exchange reaction. It has been argued in the past that the initial step for any alkane activation reaction must be the dissociative adsorption that yields

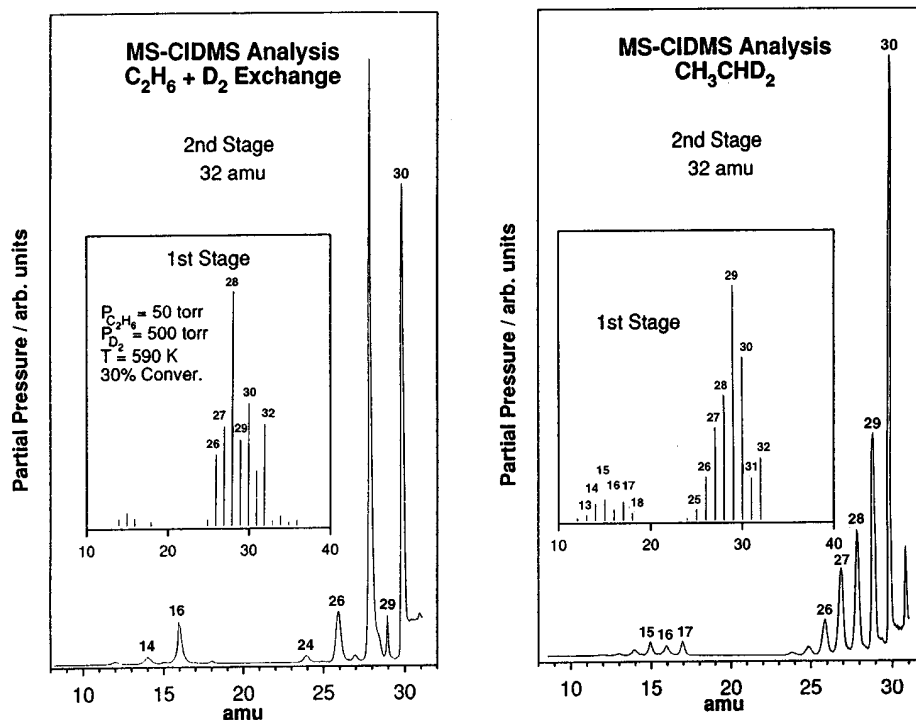


FIG. 11. Tandem mass spectrometry/collision-induced decomposition mass spectrometry (MS/MS-CID) data for both an ethane reaction mixture (left) and pure 1,1-*d*<sub>2</sub>-ethane (right). The insets show the result from the electron-impact mass spectra obtained in the first stage of the experiment, while the main frames display the data from a second mass filtering of the ions that result from the dissociation of the 32 amu ions by collision with helium atoms in the intermediate region of the instrument. Of particular importance for the purpose of the mechanistic discussion in this paper is the absence of any significant signal in the 17 amu peak of the second-stage spectrum of the mixture, because this peak is characteristic of the asymmetrically substituted *d*<sub>2</sub>-ethane. The same reaction mixture as that in Fig. 2 was used in this experiment.

the corresponding alkyl group on the surface, and that the formation of the observed monodeuterated *d*<sub>1</sub> product originates from the immediate reductive elimination of this intermediate with a surface deuterium atom (4–8). The production of perdeuteroethane (*d*<sub>6</sub>), however, requires the conversion of ethyl groups into at least one additional surface moiety. The most logical choices for such a species are ethylidene (Pt<sub>n</sub>=CHCH<sub>3</sub>) and ethylene (Pt<sub>n</sub>-CH<sub>2</sub>CH<sub>2</sub>), the products of  $\alpha$ - and  $\beta$ -hydride elimination reactions, respectively. Since direct deuteration of those intermediates would yield the corresponding CHD<sub>2</sub>CH<sub>3</sub> and CH<sub>2</sub>DCH<sub>2</sub>D gas molecules, the selective formation of the latter observed in these experiments argues for the participation of ethylene as an intermediate in the reaction.

The discussion presented above relies on the assumption that the *d*<sub>2</sub>-substituted ethane (as well as all the other isotopically substituted products) is an initial product of the reaction. Because the experiments reported here were performed in a recirculating batch reactor, however, this may not be the case. There are two possible processes by which the *d*<sub>2</sub> and other partially deuterated compounds may be formed as secondary products: (i) by readsorption and subsequent exchange of a previously single-exchanged molecule (the *d*<sub>1</sub> product, C<sub>2</sub>H<sub>5</sub>D); and (ii) by complete

exchange in an environment where the initial deuterium gas has been diluted with normal hydrogen from exchange on other molecules. Both these effects can be easily ruled out as major contributors to the products detected in this work. For one, the amount of *d*<sub>2</sub>-ethane formed by secondary exchange on *d*<sub>1</sub>-ethane can be easily estimated from the *d*<sub>1</sub> yield: if, at any time during the reaction, the fraction of *d*<sub>1</sub> in the mixture is *F*<sub>1</sub>, the fraction of *d*<sub>2</sub> produced from exchange on that *d*<sub>1</sub> is at the most *F*<sub>1</sub><sup>2</sup>. In the example presented in Table 2, *F*<sub>1</sub> = 0.028 (using the NMR data), so *F*<sub>1</sub><sup>2</sup> < 0.001, and since the actual fraction of *d*<sub>2</sub> detected in that mixture is *F*<sub>2</sub> = 0.010, we must conclude that secondary reactions contribute less than 10% to the formation of the dideuterated product. With respect to isotopic dilution, it can also be shown that it constitutes only a minor contributor in the formation of *d*<sub>5</sub>-ethane: in the example presented in Table 2, for instance, the total ethane conversion and the average number of deuterium substitutions per molecule were calculated to be about 20% and 4.54, respectively, which means that the deuterium gas at that point has been isotopically diluted with 4.5% of hydrogen. Since the fraction of the *d*<sub>6</sub> product in the mixture is *F*<sub>6</sub> = 0.087 (Table 2), the amount of *d*<sub>5</sub> originating from this dilution should be 0.045 · *F*<sub>6</sub> < 0.004; instead, the actual amount of *d*<sub>5</sub>



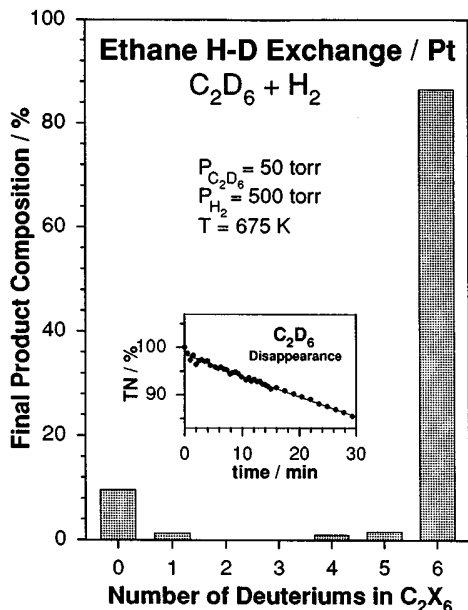


FIG. 12. Reactant disappearance curve versus reaction time (inset) and final product distribution after a 15% conversion in the exchange of 50 Torr of fully deuterated ethane with normal hydrogen over a platinum foil at 675 K. The reaction with this  $C_2D_6 + H_2$  mixture behaved in a similar fashion as when using  $C_2H_6 + D_2$ ; namely, it followed first-order kinetics and yielded a bimodal U-shaped product distribution with maxima at the single and fully substituted ethanes.

detected was  $F_5 = 0.038$ . We therefore conclude that neither secondary reactions nor isotopic dilution contribute significantly to the formation of the partially deuterated ( $d_2$  to  $d_5$ ) ethanes in our experiments.

A few research groups have attempted to determine the ratio of symmetric to asymmetric deuterium substitution on the ethane resulting from H-D exchange reactions in the past. Anderson and Kemball tried in their original work to analyze their exchange mixtures by mass spectrometry for this purpose. They used a tungsten catalyst in order to favor the mechanism responsible for  $d_1$  formation, and unsuccessfully attempted to detect the  $CHD_2^+$  fragment that would result from the cracking of  $CHD_2CH_3$  in the ionizer of the spectrometer (4). Unfortunately, no multiple exchange is operative on tungsten, so any  $d_2$  produced by that catalyst would most likely originate from a secondary reaction on the already exchanged  $d_1$  product, and would not have necessarily reflected the formation of any additional intermediate during perdeutero ethane formation. Guzzi and Ujszászi later used high-resolution mass spectrometry in the analysis of their gas samples, but obtained inconclusive results as well (24). In particular, they did not include the effect of isotope scrambling in the ionizer of the mass spectrometer in their calculations, and were also forced to compare the experimental data with limiting theoretical cases because of the lack of sensitivity in their instrument for a full analysis of the data. A detailed HR-MS analysis of

several gas mixtures was performed here with a better instrument, but the error margins involved in the calculation of the cracking patterns and the deconvolution of the data were found to be still larger than the actual signal for the  $d_2$  product (which amounts to only a few percent of the total ethane).

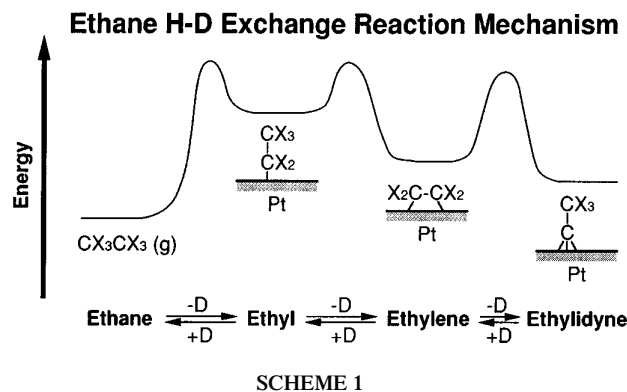
The best reported analysis of the gas products for alkane H-D exchange reactions has been that of Brown *et al.* (25). Based on results from a deuterium-NMR analysis they speculated that symmetric substitution was predominant in their samples. However, because of complications with second-order spectra given by molecules containing magnetically nonequivalent deuterium nuclei, they were not able to determine the actual product composition for the ethane mixture with this technique. Their procedure was successfully reproduced in this work, but a complete deconvolution of that data was not possible here either. The results from the  $^{13}C$ -NMR study presented above are the first to unequivocally provide the full compositional make-up of the ethane mixtures resulting from H-D exchange reactions. It is interesting to point out that even though a preference for the formation of the symmetric  $d_2$  ethane inferred in the previous work was observed here, no selectivity for any of the two possible isomers was seen in the case of  $d_4$ ; this contradicts all previous assumptions. The absence of asymmetrically substituted  $d_2$  in the mixture was further confirmed by the MS/CID-MS experiments.

Next we will discuss the implications of the formation of ethylene as an intermediate in exchange reactions on the surface chemistry of chemisorbed hydrocarbon moieties. For this we will rely on the reported chemistry of alkyl groups both in organometallic compounds and on clean single-crystal surfaces, for which a good understanding has been developed in recent years (21–23). It has been shown that by far the most favored dehydrogenation reaction on alkyl groups is a  $\beta$ -hydride elimination step (21, 33), which on platinum has to surpass an activation barrier of less than 6 kcal/mol (34), and which yields an olefin adsorbed in an  $\alpha,\beta$ -di- $\sigma$  configuration (not via a  $\pi$  interaction, as most catalysis papers assume (8, 35, 36)) (23, 37–39). Most attempts to induce the conversion of hydrocarbon surface moieties to alkylidenes (via an  $\alpha$ -hydride elimination from alkyl groups, for instance) have failed, perhaps because adsorbed ethylidene converts readily into ethylene and ethynylidyne ( $Pt_3\equiv CCH_3$ ) (40). Moreover, it appears as if the interconversion between chemisorbed ethylene and ethyl surface moieties is quite fast even at low temperatures, because extensive exchange is observed in ethylene under vacuum when deuterium atoms are coadsorbed on the surface (41–43). Finally, a new path dominates the conversion of ethylene at higher temperatures (around room temperature), namely, the formation of ethynylidyne (15), a species that is so stable that requires atmospheric hydrogen pressures and temperatures above 350 K for its removal (44).

Our catalytic results can now be understood in view of the knowledge acquired by the surface science studies. It is clear that  $\beta$ -hydride elimination still dominates over dehydrogenation at the  $\alpha$  position under the conditions of the H-D exchange reaction, because little if any  $\text{CHD}_2\text{CH}_3$  forms under most reaction conditions. Additional studies have indicated that the deuteration of the resulting ethylene, which yields the symmetrically substituted  $d_2$  ethane, requires about 13 kcal/mol on clean Pt(111) surfaces, and that it is limited by the initial conversion of the ethylene to ethyl moieties (34, 42). It is important to point out, however, that hydride elimination from the  $\alpha$ -carbon, being more activated than from the  $\beta$ -carbon, is expected to dominate at high temperatures; it has repeatedly been suggested that  $\alpha$ -H elimination precedes the more demanding hydrogenolysis reaction that produces methane (32, 45).

The detailed description of the rest of the mechanism for the production of fully deuterated alkanes still remains an open question. It was initially proposed that the selectivity between  $d_1$  and  $d_6$  production could be reflected by changing values in a probability parameter  $P$  defined as the ratio between the rates for ethyl-ethylene-ethyl cyclic surface processes and direct hydrogenation of ethyl to ethane (4). According to this model, the simultaneous production of both mono- and perdeuteroethanes on the same catalyst could be accounted for by the presence of two separate sites on the surface with different values of  $P$ . This notion was recently challenged on the grounds that the use of smooth Pt(111) single-crystal surfaces, where it is hard to conceive the presence of multiple types of active sites, leads to U-shaped product distributions similar to those seen on supported catalysts (11). It can also be argued based on the surface science results summarized above that it is not likely for ethyl-ethylene-ethyl cycles to occur repeatedly in one single residence period of the  $\text{C}_2$  fragments on the surface, because (i) the conversion of ethylene to ethyl requires much more energy than the hydrogenation of ethyl to ethane, and (ii) at the temperatures of the H-D exchange reaction it is more likely for ethylene to dehydrogenate further to ethylidyne than to convert to ethyl. Finally, the multiple stepwise exchange of hydrogens for deuteriums in adsorbed ethylene would lead to a preference for the production of symmetrically substituted  $d_4$ -ethane,  $\text{CHD}_2\text{CHD}_2$ , and this is not observed experimentally. A mechanism in which the production of all deuterium-exchanged molecules occurs on one single type of site is therefore favored here.

If all H-D exchange reactions do occur on one unique catalytic site, U-shaped product distributions such as those reported above can only be explained by a kinetic model which includes at least three different surface intermediates (46). There is by now ample evidence for the formation of alkyl and alkene intermediates in these reactions, so only one additional species is required to complete a viable mechanism. Surface science experiments are again



able to aid in the search for this third moiety. As we mentioned before, ethylene dehydrogenates quite selectively on clean platinum surfaces around room temperature to form ethylidyne (15). This reaction is in fact quite general, and takes place with other olefins and on the surface of other transition metals (23). In addition, the exchange of hydrogens for deuteriums within the methyl group of ethylidyne is faster than ethylidyne hydrogenation, at least on platinum (41, 42, 47). This means that, once formed, normal ethylidyne could easily exchange all its hydrogens to form perdeuteroethylidyne before hydrogenating (deuterating) to perdeuteroethane. Not only the rate for ethylidyne hydrogenation is roughly the same as that for ethane H-D exchange under the conditions used for the latter reaction (42, 44), but some evidence points to the presence of ethylidyne on the surface during reactions on Pt(111) (11). All this suggests that ethylidyne could indeed be the third surface species involved in the complete exchange of normal to perdeuteroethane. According to our scheme, therefore, the selectivity between  $d_1$  and  $d_6$  formation would be given by the relative rates for reductive and  $\beta$ -hydride elimination steps in ethyl groups:  $d_1$  would be produced by the direct recombination of the ethyl moieties with surface deuterium, while  $d_6$  would result from a sequence of surface steps starting with the sequential dehydrogenation of ethyl to ethylene and then to ethylidyne, continuing with the complete exchange of hydrogens for deuteriums in the methyl group of that last moiety, and ending with ethylidyne deuteration to gas-phase perdeuteroethane. These ideas are presented in Scheme 1.

We now return to discussing the kinetic data in terms of the mechanism proposed above. There are almost no arguments against the belief that the rate limiting step for most alkane activation reactions, including their H-D exchange, is the initial dissociative adsorption of the molecule (4-8). In fact, exchange reactions have been widely used as a way to estimate the activation energy for that step (1-3). However, the scatter in the reported values for the activation energy of that process (Table 3) casts some doubts on the validity of this extrapolation. Several reasons can be

TABLE 3

Comparison of Reported Kinetic Parameters for the H-D Exchange in Ethane over Platinum Catalysts

Catalyst	$E_a$ (kcal/mol)	$\log A^a$	$M^b$	Ref.
Pt film	12.5	-2.1	3.5 (410 K)	(1)
1% Pt/Cab-O-Sil	17.1	-1.4		(19)
1% Pt/SiO <sub>2</sub>	17.7	0.5		(19)
Pt black	19.0	0.0	2.6 (377–415 K)	(17)
Pt film	26.2	0.9	2.12 (573 K)	(3)
Pt(111)	19.0	2.8	3.7–4.3 (523–573 K)	(2)
Pt foil	27.1	4.0	3.2–4.6 (545–625 K)	This work

<sup>a</sup> Preexponential factor, in reaction probability per Pt atom and impinging ethane molecule.

<sup>b</sup> Average number of deuterium atoms incorporated per ethane molecule.

put forward to explain the spread in those data. For one, the problem could simply be one of experimental accuracy in the determination of reaction rates. This is particularly likely in this case, because in spite of the wide range of temperatures covered collectively by all the reports (from about 370 to 640 K), each set of experiments has in fact been performed over a narrow temperature window. Furthermore, when expressed as reaction probabilities, many of the reported preexponential factors are larger than one (Table 3); it seems as if the Arrhenius expression breaks down at some point in these calculations. Nevertheless, noticeable differences have been seen among data obtained for the same temperature range.

Another possible explanation for the inconsistency in the estimates for the activation energy of the exchange reaction could reside on the fact that this reaction is highly structure sensitive (4, 27). However, the difference in activity observed by Gucci and Sárkány between silica and Cab-O-Sil supported catalysts was associated with a change in the value of the preexponential factor, not the activation energy (27). It is interesting to notice that there is a compensation effect in the data shown in Table 3, where high activation energies seem to be associated with high preexponential factors, and that similar trends have also been reported in studies with different metals (4) and with alloys of different composition (26). We believe that this correlation between activation energies and preexponential factors may reflect at least in part changes in the coverage of the species present on the surface during reactions.

Given that the rate law of the exchange displays approximately first order dependence on ethane pressure and a negative fractional order on deuterium, it is reasonable to assume that, under the conditions of the reaction, the surface is mostly covered by deuterium, and that this adsorbed deuterium exerts an inhibiting effect on the activity of the catalysts (probably because ethane and deuterium compete for the same sites) (48). Using a Langmuir model

of adsorption, the rate law for the adsorption of the alkane (and therefore for the overall rate of the exchange) can be written as

$$R = k_{\text{ads}} \cdot P_{\text{C}_2\text{H}_6} \cdot \Theta_{\text{empty}}, \quad [1]$$

where  $\Theta_{\text{empty}}$ , which stands for the coverage of empty sites available for adsorption, can be approximated (neglecting the surface coverage of any hydrocarbon species) to

$$\Theta_{\text{empty}} = 1 - \Theta_{\text{D}}. \quad [2]$$

Assuming that the adsorbed deuterium atoms are in equilibrium with the gas-phase deuterium molecules, the surface coverage  $\Theta_{\text{D}}$  can be linked to the gas partial pressure  $P_{\text{D}_2}$  as follows:

$$\Theta_{\text{D}} = \frac{[K_{\text{D}_2} \cdot P_{\text{D}_2}]^{1/2}}{1 + [K_{\text{D}_2} \cdot P_{\text{D}_2}]^{1/2}}. \quad [3]$$

substituting Eq. [3] in Eq. [2],

$$\Theta_{\text{empty}} = 1 - \Theta_{\text{D}} = \frac{1}{1 + [K_{\text{D}_2} \cdot P_{\text{D}_2}]^{1/2}} \approx [K_{\text{D}_2} \cdot P_{\text{D}_2}]^{-1/2}, \quad [4]$$

where the term  $[K_{\text{D}_2} \cdot P_{\text{D}_2}]^{1/2}$  was assumed to be much larger than one because the surface is most likely fully covered with deuterium. Finally, substituting Eq. [4] into Eq. [1], the rate law for the reaction becomes

$$\begin{aligned} R &= [k_{\text{ads}} \cdot K_{\text{D}_2}^{-1/2}] \cdot P_{\text{C}_2\text{H}_6} \cdot P_{\text{D}_2}^{-1/2} \\ &= k_{\text{exp}} \cdot P_{\text{C}_2\text{H}_6} \cdot P_{\text{D}_2}^{-1/2}. \end{aligned} \quad [5]$$

According to this equation, the apparent activation energy measured experimentally for the exchange, which corresponds to  $k_{\text{exp}} = k_{\text{ads}} \cdot K_{\text{D}_2}^{-1/2}$ , is given by  $E_{a,\text{exp}} = E_{a,\text{ads}} - 1/2 \cdot \Delta H_{\text{ads,D}_2}$ , and therefore includes a contribution from the heat of adsorption of deuterium ( $\Delta H_{\text{ads,D}_2}$ ). This effect is particularly important, because the deuterium-pressure exponent in the rate law changes with reaction conditions, becoming less negative at lower pressures and/or higher temperatures (49); as the reaction order in  $P_{\text{D}_2}$  changes, so does the measured activation energy. An extreme of this situation can be seen at the high temperatures required to promote hydrogenolysis reactions, at which point the rate for H-D exchange is directly proportional to the pressure of deuterium, and the observed activation energy approaches a value of zero (50). Given that the heat of adsorption for hydrogen on clean platinum (111) is about -19 kcal/mol (51), a change in the deuterium order from -0.5 to 0 would correspond to a change in the apparent activation energy for the exchange of about 10 kcal/mol, the same magnitude as the spread in the reported activation barriers in Table 3.

All this suggests that the values measured experimentally for the energy barriers in alkane exchange reactions may depend on the conditions of the experiments. It should be mentioned that even though the kinetic model presented above is quite simple, it is sufficient to illustrate how those

changes may be explained. Other more sophisticated models could be developed to include factors such as the dependence of the heat of adsorption on coverages or the requirement of large ensemble sites on the surface for the activation of alkanes (52, 53), but those would still support the main points to be highlighted from the arguments put forward above, namely, that in most cases the surface of the catalyst is mostly covered with hydrogen (deuterium) during the exchange reaction, and that changes in that coverage with experimental conditions may be at least partly responsible for changes in both the orders and apparent activation energy of the reaction. It is also interesting to mention that a direct measurement of the dissociative sticking coefficient of ethane on Pt(111) yielded a value of 8.9 kcal/mol, well below any of the values reported for the exchange (54). A more detailed study on the correlation between pressures and temperature in determining reaction rates is needed to accurately establish the importance of the effect described above.

The surface coverages of the reactants on the catalytic surface not only affect the apparent activation energy of the overall conversion, but also change the final product distribution. For example, it was seen here that higher reaction temperatures lead to an increase in  $d_6$  formation at the expense of both  $d_1$  and, more noticeably,  $d_2$  (Fig. 8) on the platinum foil, and Kemball, who performed his experiments at lower temperatures, reported less  $d_6$  production (4). However, the opposite trend was seen on Pt(111) (55). The behavior on the foils may be easy to explain, because high temperatures lead to a reduction in deuterium surface coverage, and that favors decomposition reactions (ethylidyne formation) over hydrogenation steps (ethylene conversion to ethyl and to ethane). Indeed, on clean Pt(111), only the rate for ethylene H–D exchange (which involves the formation of an ethyl intermediate) correlates with the coverage of coadsorbed deuterium; the rate for ethylidyne formation from ethylene is independent of that coverage (43). In any case, the changes in product distribution with reaction temperature reported in the studies cited above were not significant, a fact that leads to the conclusion that the apparent activation energy for all of the individual deuterium substituted products is about the same. Also, most of these studies were carried out under conditions where H–D exchange was the only reaction observed; no hydrogenolysis was reported in most cases. Harder to understand are the changes in selectivity observed over time during a given run (Fig. 7). The composition of the surface must change slowly during the course of the reaction, perhaps because a small amount of carbonaceous deposits builds up over time. The presence of hydrocarbon species on the surface does affect the selectivity between hydrogenation and dehydrogenation reactions. On clean Pt(111) and under vacuum, for instance, the initial selective formation of ethylene from ethyl at low coverages is offset by the takeover of ethane

desorption near saturation (19, 56). These changes are believed to be associated with the different ensemble sizes required for the different reactions (3, 57–59).

Finally, ethane was used in this study as representative of a broader family of compounds, namely, that of alkanes. We believe that the conclusions regarding the mechanism of H–D exchange reactions reached here are quite general, and can be extrapolated to other systems. For one, the preference of alkyl groups to dehydrogenate at the  $\beta$  position has been shown to occur on a wide variety of alkyl surface groups (22, 23, 60), and the formation of alkylidynes from larger olefins has also been reported (22, 61, 62). In any case, the type of experiments reported here with ethane can be easily extended to more complex molecules. In particular, the additive nature of the shifts in the  $^{13}\text{C}$ -NMR signal with deuterium substitution allows for the straightforward assignment the spectral features in other cases (30). Also, this analysis does not require the use of  $^{13}\text{C}$ -isotopically enriched reactants, normal samples can be used as long as longer data-acquisition times (several hours) are used for the NMR spectra; this was successfully done here for the case of ethane. We expect the use of  $^{13}\text{C}$ -NMR to analyze mixtures of isotopically-substituted samples to become more common in the near future.

## 5. CONCLUSIONS

The kinetics of the catalytic exchange of hydrogen atoms for deuteriums in ethane over a platinum foil was studied. The reaction displayed an activation energy of 27.1 kcal/mol, and  $-0.55$  and  $1.04$  orders with respect to the deuterium and ethane partial pressures, respectively. The product distribution displayed a U-shape in all cases, with maxima at one and six deuterium atoms per ethane molecule. A more complete analysis of the reaction mixture by  $^{13}\text{C}$ -NMR indicated that there is a preference for the formation of the symmetric  $\text{CH}_2\text{DCH}_2\text{D}$   $d_2$ -ethane, but no selectivity between symmetric and asymmetric substitutions in the  $d_4$ -products was seen. These results point to a mechanism for the multiple H–D exchange in alkanes involving alkyl and olefinic intermediates. Additional kinetic arguments suggest the formation of a third intermediate which, based on surface science results, was argued to be alkylidyne.

Several analytical methods were also tested for the analysis of gas-phase isotopically substituted alkane mixtures. It was determined that high-resolution mass spectrometry is unreliable for this purpose, especially in cases such as those found in H–D catalytic exchange reactions where the gas sample is mostly composed of mono- and perdeuteroalkanes. Analysis by  $^{13}\text{C}$ -NMR, on the other hand, was found to be straightforward, and ideally suited for the separation of symmetrically and asymmetrically deuterium-substituted compounds. Tandem MS/CID-MS was also helpful for this endeavor in certain specific cases.

## ACKNOWLEDGMENTS

We want to thank Drs. Dan Borchardt and Richard Kondrat for their help with the NMR and the high-resolution mass spectrometer, respectively. We are also grateful to Professor Wilfred T. Tysoe for providing us with most of the labeled ethane samples used for mass spectrometry and NMR calibration. This work was supported by National Science Foundation (NSF) Grant CHE-9222164. Financial aid for Alfonso Loaiza was provided by La Universidad de Los Andes-Mérida, Venezuela.

## REFERENCES

- Bond, G. C., "Catalysis by Metals." Academic Press, London, 1962.
- Gates, B. C., Katzer, J. R., and Schuit, G. C. A., "Chemistry of Catalytic Processes." McGraw-Hill, New York, 1979.
- Zaera, F., and Somorjai, G. A., in "Hydrogen Effects in Catalysis; Fundamental and Practical Applications" (Z. Paal and P. G. Menon, Eds.), p. 425. Dekker, New York, 1988.
- Anderson, J. R., and Kemball, C., *Proc. R. Soc. London Ser. A* **223**, 361 (1954).
- Guczi, L., Sárkány, A., and Tétényi, P., *J. Chem. Soc. Faraday Trans. 1* **70**, 1971 (1974).
- Anderson, J. R., *Rev. Pure Appl. Chem.* **7**, 165 (1957).
- Taylor, T. I., in "Catalysis" (P. H. Emmett, Ed.), Vol. 5, p. 256. Reinhold, New York, 1957.
- Kemball, C., *Adv. Catal. Relat. Subj.* **11**, 223 (1959).
- Frennet, A., and Lienard, G., *Surf. Sci.* **18**, 80 (1969).
- Frennet, A., Crucq, A., Degols, L., and Liénard, G., *Acta Chim. Acad. Sci. Hung.* **111**, 499 (1982).
- Zaera, F., *J. Phys. Chem.* **89**, 3211 (1985).
- Demuth, J. E., and Ibach, H., *Surf. Sci.* **78**, L238 (1978).
- Kesmodel, L. L., Dubois, L. H., and Somorjai, G. A., *J. Chem. Phys.* **70**, 2180 (1979).
- Dubois, L. H., Castner, D. G., and Somorjai, G. A., *J. Chem. Phys.* **72**, 5234 (1980).
- Skinner, P., Howard, M. W., Oxtan, I. A., Kettle, S. F. A., Powell, D. B., and Sheppard, N., *J. Chem. Soc. Faraday Trans.* **77**, 1203 (1981).
- George, P. M., Avery, N. R., Weinberg, W. H., and Teble, F. N., *J. Am. Chem. Soc.* **105**, 1393 (1983).
- Gates, G. A., and Kesmodel, L. L., *Surf. Sci.* **124**, 68 (1983).
- Zaera, F., and Hall, R. B., *Surf. Sci.* **180**, 1 (1987).
- Zaera, F., *Surf. Sci.* **219**, 453 (1989).
- Zaera, F., *J. Phys. Chem.* **94**, 5090 (1990).
- Zaera, F., *Acc. Chem. Res.* **25**, 260 (1992).
- Zaera, F., *J. Mol. Catal.* **86**, 221 (1994).
- Zaera, F., *Chem. Rev.* **95**, 2651 (1995).
- Guczi, L., and Ujszászi, *React. Kinet. Catal. Lett.* **8**, 489 (1978).
- Brown, R., Kemball, C., Oliver, J. A., and Sadler, I. H., *J. Chem. Res.*, M-3201 and S-274 (1985).
- Guczi, L., and Karpinski, Z., *J. Catal.* **56**, 438 (1979).
- Guczi, L., and Sárkány, A., *J. Catal.* **68**, 190 (1981).
- Wesener, J. R., Moskau, D., and Gunter, H., *J. Am. Chem. Soc.* **107**, 7307 (1985).
- Alei, M., Jr., and Wageman, W. E., *J. Chem. Phys.* **68**, 783 (1978).
- Loaiza, A., Borchardt, D., and Zaera, F., to appear.
- Loaiza, A., and Zaera, F., to appear.
- Babernics, L., Gucci, L., Matusek, K., Sárkány, A., and Tétényi, P., in "Proceedings, 6th International Congress on Catalysis" (G. C. Bond, P. B. Wells, and F. C. Tompkins, Eds.), Vol. 1, p. 456. The Chemical Society, London, 1976.
- Zaera, F., *J. Am. Chem. Soc.* **111**, 8744 (1989).
- Zaera, F., *J. Phys. Chem.* **94**, 8350 (1990).
- Burwell, R. L., Jr., *Acc. Chem. Res.* **2**, 289 (1969).
- Clarke, J. K. A., and Rooney, J. J., *Adv. Catal.* **25**, 125 (1976).
- Steininger, H., Ibach, H., and Lehwald, S., *Surf. Sci.* **117**, 685 (1982).
- Horsley, J. A., Stöhr, J., and Koestner, R. J., *J. Chem. Phys.* **83**, 3146 (1985).
- Stuve, E. M., and Madix, R. J., *J. Phys. Chem.* **89**, 3183 (1985).
- Janssens, T. V. W., and Zaera, F., submitted for publication.
- Janssens, T. V. W., and Zaera, F., *Surf. Sci.*, **344**, 77 (1995).
- Zaera, F., *Langmuir*, **12**, 88 (1996).
- Stone, D., Hemminger, J. C., Janssens, T. V. W., and Zaera, F., to appear.
- Davis, S. M., Zaera, F., Gordon, B. E., and Somorjai, G. A., *J. Catal.* **92**, 240 (1985).
- Sinfelt, J. H., *Adv. Catal.* **23**, 223 (1973).
- Miyahara, K., *J. Res. Inst. Catal. Hokkaido Univ.* **4**, 43 (1956).
- Wieckowski, A. J., Rosasco, S. D., Salaita, G. N., Hubbard, A., Bent, B. E., Zaera, F., Godbey, D., and Somorjai, G. A., *J. Am. Chem. Soc.* **107**, 5910 (1985).
- Frennet, A., in "Prospectives in Catalysis, (Proc. 12th Swedish Symp. Catal.)" (R. Larsson, Ed.), p. 49. CWK Gleerup, 1981.
- Tétényi, P., Gucci, L., and Paál, Z., *Acta Chim. Acad. Sci. Hung.* **83**, 37 (1974).
- Davis, S. M., and Somorjai, G. A., *J. Phys. Chem.* **87**, 1545 (1983).
- Poelsema, B., Mechttersheim, G., and Comsa, G., *Surf. Sci.* **111**, 519 (1981).
- Frennet, A., in "Hydrogen Effects in Catalysis; Fundamental and Practical Applications" (Paál and P. G. Menon, Eds.), p. 399. Dekker, New York, 1988.
- Frennet, A., Lienard, G., Crucq, A., and Degols, L., *Surf. Sci.* **80**, 412 (1979).
- Rodriguez, J. A., and Goodman, D. W., *J. Phys. Chem.* **94**, 5342 (1990).
- Zaera, F., Ph. D. Thesis, University of California, Berkeley, 1984.
- Hoffmann, H., Griffiths, P. R., and Zaera, F., *Surf. Sci.* **262**, 141 (1992).
- Thomas, J. M., and Thomas, W. J., "Introduction to the Principles of Heterogeneous Catalysis." Academic Press, London, 1967.
- Sachtler, W. M. H., and van Santen, R. A., *Adv. Catal.* **26**, 69 (1977).
- Sinfelt, J. H., and Cusumano, J. A., in "Advanced Materials in Catalysis" (J. J. Burton, and R. L. Garten, Eds.), p. 1. Academic Press, New York, 1977.
- Tjandra, S., and Zaera, F., *J. Am. Chem. Soc.* **117**, 9749 (1995).
- Avery, N. R., and Sheppard, N., *Proc. R. Soc. London Ser. A* **405**, 1 (1986).
- Bent, B. E., Mate, C. M., Crowell, J. E., Koel, B. E., and Somorjai, G. A., *J. Phys. Chem.* **91**, 1493 (1987).